Representations of the Temperature Correlation Effect in Lattice Calculations

Alain Hébert*[1]

Ecole Polytechnique de Montréal, P.O. Box 6079 station ``Centre-Ville", Montréal Qc. CANADA H3C 3A7

*[1]alain.hebert@polymtl.ca

Received 17 January 2014; Accepted 19 March 2014; Published 27 June 2014

Abstract

We are investigating the accuracy of various techniques for representing the temperature profile inside a fuel pin. The simplest approach consists in replacing the temperature profile by a single effective temperature. Here, we propose to treat explicitly the temperature gradient in fuel pins, using a subgroup self-shielding model together with various representations of the temperature correlation effect between different isotopes and fuel regions. We conclude that it is now possible to use an explicit representation of the temperature distribution in routine lattice calculations, without the introduction of an effective temperature.

Keywords

Lattice Calculation; Resonance Self-shielding; Doppler Effect; Computational Schemes

Introduction

Until recently, the recommended way to represent a temperature profile within the fuel pin was to replace this distribution with a uniform *effective* temperature, defined in such a way to preserve the integrated absorption rate within fuel (see de Kruijf and Janssen, 1996). This effective fuel temperature is an important parameter for the calculation of the Doppler effect and of the neutronic feedback during power transients. The effective fuel temperature is generally obtained as a weighted average of the temperatures in the fuel zones. Two simple theoretical expressions for this weighted averaged are proposed in the literature: the *chord-averaged* and the *volume-averaged* values. However, using such simple expressions has many drawbacks. These expressions are valid if the number density of the resonant isotope is almost constant in the fuel pin, which is only true for ^{238}U. In some cases, the effective temperature is found to be energy-dependent, a situation difficult to handle in many lattice codes. Finally, most effective temperature models are assuming a parabolic shape of the temperatures, a situation valid only under steady-state conditions. Modern lattice designs involve the introduction of different fuel pins with various isotopic contents, with or without burnable poisons. In some cases, the burnable poison is mixed with depleted fuel, leading to lower temperature pins. It is not always possible to find a unique effective temperature for all occurrences of a given isotope in the lattice, so that the accurate representation of temperature gradient effects in fuel cannot be avoided.

A more straightforward approach to represent a temperature profile is to divide the fuel into onion rings and to assign a different temperature to each of them. Most existing lattice codes cannot use this approach because of the strong correlation existing between different cross-section sets of a unique resonant isotope at different temperatures. Without special treatment, a lattice code assumes no correlation between the resonances in different cross-section sets, which is false for a unique resonant isotope at different temperatures.

However, using a modern self-shielding treatment based on the subgroup approach opens the way to the correct representation of these temperature correlation effects.

A first model for representing the temperature correlation effect was first implemented in the lattice code ECCO, dedicated to the study of fast reactor lattices (see Grimstone, Tullett and Rimpault, 1990). This model, implemented within the subgroup algorithm, is assuming a *full correlation* between different cross-section sets of a unique resonant isotope. Another full correlation model was also proposed by Perruchot (1996) in the context of the Sanchez-Coste method of the Apollo2 code. These

models are interesting as they can be used within coarse energy groups, such as those available in XMAS–172g and SHEM–281g. The full correlation model in the context of subgroup equations is also presented in Sect. II B of a technical paper by Hébert (2009).

Recently, we have proposed a new self-shielding method consistent with the introduction of a finer energy mesh, using as many as 295 energy groups (see Hébert, 2009). Using so many groups makes possible a simplification of the Ribon extended model, already presented by Hébert (2004), and the introduction of a new cross section correlation model with the capability to represent a temperature gradient in fuel. The same correlation model is also able to represent the *mutual shielding effect* between different resonant isotopes, although this effect is almost vanishing with a 295–group energy mesh. The proposed self-shielding method is referred as the *subgroup projection method* (SPM). The paper will describe the different correlation models, together with their implementation details.

Theory

The self-shielding calculations are kept apart from the main flux calculation, thanks to the Livolant-Jeanpierre factorization presented in Sect. 4.2.3 of *Applied Reactor Physics* (Hébert, 2009). Our study is based on two types of subgroup-based self-shielding methods. The first method, used with XMAS–172g and SHEM–281g meshes, is the Statistical slowing-down (ST) subgroup method, as introduced in Sect. 4.2.5 also of *Applied Reactor Physics*. It is based in *physical probability tables* where the table corresponding to the total cross section in an energy group is computed so as to match the numerical integration results with the tabulated values for specific values of the microscopic dilution cross section in this group.

The second method, used with SHEM–295g mesh, is the Subgroup Projection Method (SPM) introduced in Hébert's technical paper (2009). The original computing properties of the SPM can be summarized as follows:

1. The SPM is a subgroup approach based on CALENDF–type probability tables (see Hébert and Coste, 2002).
2. The self-shielding calculations are limited to energies above 4.63 eV. The SPM is used below 11.14 keV and the ST approach with physical probability tables is used above.
3. The new cross section correlation model can effectively represent both *mutual shielding effects* and *temperature gradient effects* in fuel, *without* introducing additional CPU costs other than those associated with the use of 151 energy groups.
4. Using as many as 151 energy groups between 4.63 eV and 11.14 keV, the s*uper-homogénéisation* (SPH) treatment of the self-shielded cross sections is not required. However, the SPH treatment is kept in the remaining groups with a lethargy width greater than 0.1.
5. The SPM can represent isotopic correlation effects in three different ways. A non-correlation approximation is first available in the case where resonances belonging to different isotopes are overlapping in a statistical way. A full-correlation model, similar to the model used in the ECCO lattice code, is available if different cross section sets are corresponding to the same isotope at different temperatures (see Grimstone, Tullett and Rimpault, 1990). Finally, a general correlation model is available with the capability to represent any level of correlation, from no correlation to full correlation.

The simplified transport equation presented in Eq. (29) of Hébert's technical paper (2005) can be generalized to heterogeneous situations and used to describe a lattice with a unique resonant isotope. Here, we consider a simplified transport equation over a coarse group g where the non-resonant cross sections are assumed to be constant in lethargy. We write

$$\Omega\cdot\nabla\varphi(r,u,\Omega)+\Sigma(r,u)\varphi(r,u,\Omega) = \frac{1}{4\pi}\left[\Sigma_s^+(r)\mathbf{r}\{\varphi(r,u)\}\right] \quad (1.1)$$

where

$\varphi(r,u,\Omega)$ = fine structure function of the neutron flux

$\Sigma(r,u)$ = macroscopic total cross section of the resonant isotope at position $\boldsymbol{r}$

$\Sigma_s^+(r)$ = macroscopic P_0 scattering cross section of the non--resonant isotopes at position $\boldsymbol{r}$

$N^*(r)$ = number density of the resonant isotope at position $\boldsymbol{r}$

$\mathbf{r}\{\varphi(r,u)\}$ = microscopic slowing-down ope-rator for nuclear reactions with a single heavy isotope.

The *statistical slowing-down* (ST) model is based on the assumption that the resonances of the heavy isotope are narrow, numerous and statistically distributed in group *g*. This model is more accurate than the *narrow resonance* (NR) model where the resonances are assumed to be isolated, which is not the case at high neutron energy. The heavy isotope's slowing-down operator is written with the ST model as

$$\mathbf{r}\{\varphi(r,u)\} = \langle \sigma_s^*(r)\varphi(r)\rangle_g \quad \text{if} \quad u_{g-1} \le u < u_g \tag{1.2}$$

where

$$\langle \sigma_s^*(r)\varphi(r)\rangle_g = \frac{1}{\Delta u_g}\int_{u_{g-1}}^{u_g} du\, \sigma_s^*(r,u)\varphi(r,u). \tag{1.3}$$

In coarse energy group *g*, we define a probability table of order K as $\{\omega_k, \sigma_k^*(r), \sigma_{s,k}^*(r), k=1,K\}$. We next define $\varphi_k(r)$ as the space-dependent flux in subgroup *k*. Using Eq. (1.2), the subgroup form of Eq. (1.1) is written

$$\begin{aligned}&\Omega\cdot\nabla\varphi_k(r,\Omega)+\left[\Sigma^+(r)+\Sigma_k(r)\right]\varphi_k(r,\Omega)\\ &=\frac{1}{4\pi}\left[\Sigma_s^+(r)+N^*(r)\sum_{\ell=1}^{K}\omega_\ell\,\sigma_{s,\ell}^*(r)\varphi_\ell(r)\right]\end{aligned} \tag{1.4}$$

where

$\Sigma^+(r)$ = macroscopic total cross sections of the non-resonant isotopes at position $\boldsymbol{r}$

$\Sigma_k(r)$ = macroscopic total cross section of the resonant isotope in subgroup *k*

$\sigma_{s,\ell}^*(r)$ = microscopic P_0 scattering cross section of the resonant isotope in subgroup ℓ.

Equation (1.4) can be solved using an iterative approach. Scattering reduction consists to include the term $N^*(r)\omega_k\sigma_{s,k}^*(r)\varphi_k(r)$ in the LHS in order to reduce the total number of fixed point iterations. Eq. (1.4) is therefore replaced by

$$\begin{aligned}&\Omega\cdot\nabla\varphi_k(r,\Omega)+\left[\Sigma^+(r)+\Sigma_k(r)\right]\varphi_k(r,\Omega)\\ &-\frac{1}{4\pi}N^*(r)\omega_k\,\sigma_{s,k}^*(r)\varphi_k(r)\\ &=\frac{1}{4\pi}\left[\Sigma_s^+(r)+N^*(r)\sum_{\substack{\ell=1\\ \ell\neq k}}^{K}\omega_\ell\,\sigma_{s,\ell}^*(r)\varphi_\ell(r)\right].\end{aligned} \tag{1.5}$$

Equation (1.5) is solved iteratively using the following fixed-point approach:

$$\begin{aligned}&\Omega\cdot\nabla\varphi_k^{(n)}(r,\Omega)+\left[\Sigma^+(r)+\Sigma_k(r)\right]\varphi_k^{(n)}(r,\Omega)\\ &-\frac{1}{4\pi}N^*(r)\omega_k\,\sigma_{s,k}^*(r)\varphi_k^{(n)}(r)=\frac{1}{4\pi}S_k^{(n)}(r)\end{aligned} \tag{1.6}$$

where the space-dependent sources at iteration *(n)* are computed from the subgroup flux unknowns of the previous iteration using

$$S_k^{(n)}(r)=\Sigma_s^+(r)+N^*(r)\sum_{\substack{\ell=1\\ \ell\neq k}}^{K}\omega_\ell\,\sigma_{s,\ell}^*(r)\varphi_\ell^{(n-1)}(r). \tag{1.7}$$

If a second resonant isotope is admixed, or if the same resonant isotope is admixed with a different temperature, we represent this new instance as $b \neq a$ so that Eq. (1.6) must be updated to take into account the effects of *b*. The simplest approximation consists of neglecting any correlation between *a* and *b*. In this case, we write

$$\begin{aligned}&\Omega\cdot\nabla\varphi_k^{a,(n)}(r,\Omega)\\ &+\left[\Sigma^+(r)+\Sigma_k^a(r)+\Sigma_k^{b/a}(r)\right]\varphi_k^{a,(n)}(r,\Omega)\\ &-\frac{1}{4\pi}N^{*a}(r)\omega_k^a\,\sigma_{s,k}^{*a}(r)\varphi_k^{a,(n)}(r)=\frac{1}{4\pi}S_k^{a,(n)}(r)\end{aligned} \tag{1.8}$$

where

$$\Sigma_k^{b/a}(r)=\frac{\sum_{\ell=1}^{K_b}\omega_\ell^b\,\Sigma_\ell^b(r)\varphi_\ell^{b,(n-1)}(r)}{\sum_{\ell=1}^{K_b}\omega_\ell^b\,\varphi_\ell^{b,(n-1)}(r)} \tag{1.9}$$

and where the source term is now written as

$$\begin{aligned}S_k^{a,(n)}(r)=&\Sigma_s^+(r)+N^{*a}(r)\sum_{\substack{\ell=1\\ \ell\neq k}}^{K_a}\omega_\ell^a\,\sigma_{s,\ell}^{*a}(r)\varphi_\ell^{a,(n-1)}(r)\\ &+N^{*b}(r)\sum_{\ell=1}^{K_b}\omega_\ell^b\,\sigma_{s,\ell}^{*b}(r)\varphi_\ell^{b,(n-1)}(r).\end{aligned} \tag{1.10}$$

Equation (1.9) is the component of total cross section belonging to isotope *b* that should be included in the *k*–th subgroup of isotope *a*, taking into account any mutual interaction effect. Here, all mutual interaction effects are neglected. Consequently, the RHS of Eq. (1.9) is independent of index *k* and superscript *a*.

The above approximation is expected to be acceptable, provided that the energy group widths are small enough in the energy domains with overlapping resonances. The approximation is known to fail if isotopes *a* and *b* are corresponding to the same isotope at different temperatures. In this case, a *full-correlation* approximation can be written, as used in the ECCO lattice code (see Grimstone, Tullett and Rimpault,

1990):

$$\Omega\cdot\nabla\varphi_k^{a,(n)}(r,\Omega) + \left[\Sigma^{+}(r)+\Sigma_k^a(r)+N^{*b}(r)\sigma_k^a(r)\right]\varphi_k^{a,(n)}(r,\Omega) - \frac{1}{4\pi}N^{*a}(r)\,\omega_k^a\,\sigma_{s,k}^{*a}(r)\,\varphi_k^{a,(n)}(r) = \frac{1}{4\pi}S_k^{a,(n)}(r). \quad (1.11)$$

The full-correlation approximation consists to process each ring of fuel as a specific self-shielding problem, assuming that the neighboring rings are containing the resonant isotope at the *same temperature* as the temperature being processed. This approximation causes full-correlation in probability tables because all rings have the same resonant microscopic cross sections. Each ring is self-shielded at its exact temperature.

Finally, a general correlation model can be set, using the *correlated weight matrix* $\omega_{k,\ell}^{ab}$ previously introduced and obtained in Sect. II.B. of Hébert's technical paper (2005). In this case, Eq. (1.8) is used with Eq. (1.9) replaced by

$$\Sigma_k^{b/a}(r) = \frac{\sum_{\ell=1}^{K_b}\omega_{k,\ell}^{ab}\,\Sigma_\ell^b(r)\,\varphi_\ell^{b,(n-1)}(r)}{\sum_{\ell=1}^{K_b}\omega_{k,\ell}^{ab}\,\varphi_\ell^{b,(n-1)}(r)}. \quad (1.12)$$

The numerical effect of the correlation can be removed and Eq. (8) can be obtained by writing $\omega_{k,\ell}^{ab}=\omega_k^a\,\omega_\ell^b$. Similarly, a full correlation model can be obtained by writing $\omega_{k,\ell}^{ab}=\omega_k^a\,\delta_{k,\ell}$ where $\delta_{k,\ell}$ is the *Delta Kronecker function*.

Similar expressions can be written for the flux $\varphi_k^{b,(n)}(r,\Omega)$ in isotope *b*. Moreover, the overall approach can be generalized to an arbitrary number of admixed resonant isotopes.

The *k*–th subgroup flux and reaction rates can be averaged over each resonant region *i* using

$$\varphi_{i,k}=\frac{1}{V_i}\int_{V_i}d^3r\,\varphi_k(r) \quad (1.13)$$

and

$$\sigma_{\rho,i,k}=\frac{1}{V_i\,\varphi_{i,k}}\int_{V_i}d^3r\,\sigma_{\rho,k}(r)\,\varphi_k(r) \quad (1.14)$$

where V_i is the volume of the *i*–th resonant region.

After convergence of the subgroup flux unknowns, it is possible to compute the integrated flux $\langle\varphi_i\rangle_g$ and reaction rate $\langle\sigma_{\rho,i}\,\varphi_i\rangle_g$ for reaction ρ in region *i* using

$$\langle\varphi_i\rangle_g=\sum_{k=1}^{K}\omega_k\,\varphi_{i,k} \quad (1.15)$$

and

$$\langle\sigma_{\rho,i}\,\varphi_i\rangle_g=\sum_{k=1}^{K}\omega_k\,\sigma_{\rho,i,k}\,\varphi_{i,k} \quad (1.16)$$

where the probability table of group *g* has been used.

Numerical Results

We have based our validation study on a modified Rowlands pin-cell case (see Rowlands *et al.*, 1999) featuring a temperature gradient in fuel, as depicted in Fig 1. The comparisons were made for a light-water, MOX (UPuO2 fuelled), reactor pin-cell without leakage. The effects of changes in temperature were investigated in order to examine the consistency of temperature calculation methods.

The one-neutron source benchmark is limited to the resolved energy domain where it is possible to precisely define the resonant cross sections. The scattering kernel is assumed to be purely elastic.

Cross sections were defined in the resolved energy domain and distributed over SHEM–295 energy groups 56 to 206, located between 4.63 eV and 11.14 keV. A 1.0 n/cm³ · s source was placed in group number 56, located between 9.1188 keV and 11.138 keV and the absorption rates are computed in the remaining energy groups.

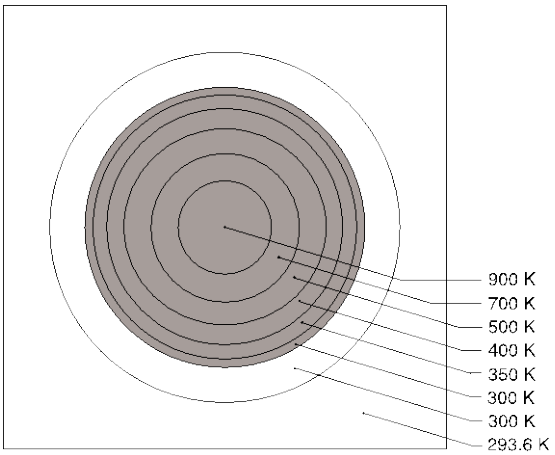

FIG. 1 TEMPERATURE GRADIENT IN A MOX PINCELL

Cross section libraries in PENDF and Draglib formats were build from scratch with NJOY release 99.259+upnea027. Draglib–formatted data is including temperature–dependent Autolib data for all resonant isotopes between 4.63 eV and 11.14 keV. The elementary lethargy width of the Autolib data is 5×10^{-4}.

Two computer codes have been used to perform these tests:

1. A computer code, named CESCOL, makes it possible to solve a fixed-source slowing-down equation using a P_0 elastic slowing-down operator for a mixture of heavy (resonant) isotopes in the resolved energy domain (see Hébert and Marleau, 1991). Heterogeneous cases can also be treated using collision probability (CP) techniques and used to generate reference solutions. CESCOL is implemented as a stand-alone module in a non-official version of DRAGON. Fine-group cross sections used by CESCOL are recovered in Autolib format from the Draglib database. Note that the same Autolib data is also used to compute the CALENDF probability tables used in the SPM subgroup model.
2. A self-shielding operator was written in the DRAGON Version 4.0.2 lattice code (see Marleau, Hébert and Roy, 2006 and Hébert, 2006) based on the SPM subgroup model. Self-shielded cross sections are obtained for a coarse energy grid and used in the existing CP flux solution operators. Consistency is emphasized by using the same CP calculation operator in both heterogeneous CESCOL and lattice code calculations.

We studied the absorption rates for the resonant isotopes in energy groups 56 to 206 and reported the discrepancies between CESCOL and lattice code. The main purpose of the numerical tests was to compare the proposed self-shielding methodology with reference

TABLE 1 SUMMARY OF MOX (FUEL 1) ONE-NEUTRON SOURCE BENCHMARK. USE OF SHEM—295

	effective temperature[a]	temperature gradient: no correlation	temperature gradient: full correlation (ECCO)	temperature gradient: correlated weight matrices (SPM)
ϵ^{int} (%)	0	5.700	0.327	0.280
$\bar{\epsilon}$ (%)	0.908	7.246	1.093	0.698
ϵ^{max} (%)	4.025	51.417	7.318	3.319
in group	126	100	131	124
^{235}U ϵ^{int} (%)	0.375	-4.009	-0.418	0.163
^{238}U ϵ^{int} (%)	-0.206	11.884	-0.204	0.245
^{238}Pu ϵ^{int} (%)	0.123	-3.610	-1.155	0.050
^{239}Pu ϵ^{int} (%)	0.202	1.808	0.680	0.416
^{240}Pu ϵ^{int} (%)	-0.437	4.501	1.032	0.021
^{241}Pu ϵ^{int} (%)	0.265	-2.435	0.971	0.134
^{242}Pu ϵ^{int} (%)	0.141	0.944	0.295	0.180
^{241}Am ϵ^{int} (%)	0.304	-2.250	1.423	0.176
^{238}U ϵ^{int} (%)				
shell 1	-5.318	7.450	0.126	0.775
shell 2	-3.912	8.529	1.261	0.766
shell 3	0.372	20.448	0.555	1.716
shell 4	5.023	21.519	-0.542	0.729
shell 5	8.914	31.739	-2.419	-1.832
shell 6	10.398	3.612	-3.218	-2.630

[a] Effective temperature set to T_{eff} = 628.95 K (ϵ^{int} = 0).

TABLE 2 SUMMARY OF MOX (FUEL 1) ONE-NEUTRON SOURCE BENCHMARK. USE OF XMAS–172

	effective temperature[a]	temperature gradient: no correlation	temperature gradient: full correlation (ECCO)
ϵ^{int} (%)	0	18.556	0.890
$\bar{\epsilon}$ (%)	2.744	14.051	3.084
ϵ^{max} (%)	10.775	61.209	11.781
in group	69	75	73
^{235}U ϵ^{int} (%)	0.846	-12.498	0.281
^{238}U ϵ^{int} (%)	-2.336	48.223	-2.094
^{238}Pu ϵ^{int} (%)	-1.443	-10.339	-1.984
^{239}Pu ϵ^{int} (%)	0.393	0.821	1.805
^{240}Pu ϵ^{int} (%)	4.492	12.221	8.606
^{241}Pu ϵ^{int} (%)	3.878	-8.723	3.767
^{242}Pu ϵ^{int} (%)	-2.768	-2.095	3.419
^{241}Am ϵ^{int} (%)	4.738	-7.744	4.165
^{238}U ϵ^{int} (%)			
shell 1	-6.172	24.247	-3.381
shell 2	-5.566	42.356	-3.781
shell 3	-1.884	107.491	-1.435
shell 4	1.778	86.643	0.524
shell 5	4.388	95.434	0.454
shell 6	5.029	12.078	-0.205

[a] Effective temperature set to T_{eff} = 449.25 K (ϵ^{int} = 0).

TABLE 3 SUMMARY OF MOX (FUEL 1) ONE-NEUTRON SOURCE BENCHMARK. USE OF SHEM–281

	effective temperature[a]	temperature gradient: no correlation	temperature gradient: full correlation (ECCO)
ϵ^{int} (%)	0	26.602	1.069
$\bar{\epsilon}$ (%)	3.426	22.001	3.119
ϵ^{max} (%)	16.286	61.006	18.866
in group	89	85	89
^{235}U ϵ^{int} (%)	-0.386	-9.676	-0.718
^{238}U ϵ^{int} (%)	-2.703	61.691	-1.406
^{238}Pu ϵ^{int} (%)	0.346	-4.853	0.073
^{239}Pu ϵ^{int} (%)	2.130	2.986	2.937
^{240}Pu ϵ^{int} (%)	2.256	8.999	5.277
^{241}Pu ϵ^{int} (%)	1.384	-6.519	1.068
^{242}Pu ϵ^{int} (%)	-1.194	-0.260	-0.265
^{241}Am ϵ^{int} (%)	2.830	-6.727	2.488
^{238}U ϵ^{int} (%)			
shell 1	-8.504	37.085	-2.256
shell 2	-4.954	56.041	-1.737
shell 3	0.718	115.593	-0.155
shell 4	4.546	94.756	0.496
shell 5	6.345	105.304	-0.295
shell 6	5.675	39.758	-1.746

[a] Effective temperature set to T_{eff} = 521.3 K (ϵ^{int} = 0).

CESCOL calculations. The corresponding numerical results corresponding to meshes SHEM–295, XMAS–172 and SHEM–281 are presented in Tables 1 to 3, respectively. We are reporting global error values for maximum ϵ^{max}, averaged $\bar{\epsilon}$ and integrated error ϵ^{int} isotopic and spatially-dependent ϵ^{int} values. This overall exercise was repeated with legacy SHEM–281g and XMAS–172g energy meshes. The percent errors on absorption rates are plotted in Fig. 2. Meshes XMAS–

172 and SHEM–281 are too coarse to enable use of CALENDF–based SPM. Consequently, the subgroup equations were solved using physical probability tables, as explained in Sect. 4.2.4 of *Applied Reactor Physics* (Hébert, 2009). Mesh SHEM–295, on the other hand, is fully compatible with the SMP and with the correlated weight matrix calculation presented in this paper.

An important observation is related to the use of the SPM–type general correlation model. The application of the SPM–type general correlation model permits to reduce the maximum error by a factor of two. It is important to note that the correlation model introduces no additional CPU costs in the subgroup solution, so that it can be left active in all situations. Both ECCO– and SPM–type correlation models permit to treat correctly the fuel temperature coefficient in presence of temperature gradient.

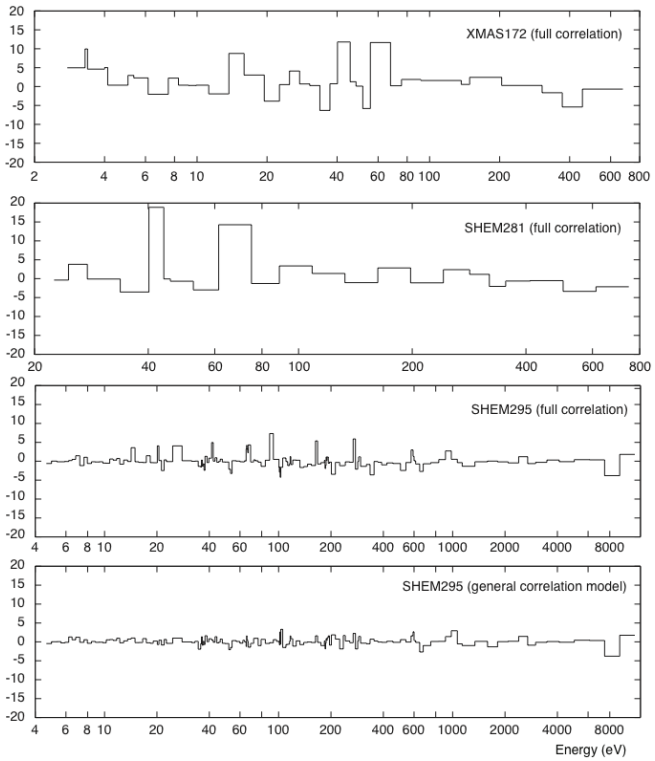

FIG. 2 PERCENT ERRORS ON ABSORPTION RATES

Conclusions

Current self-shielding approaches existing in legacy production codes are generally based on the effective temperature approximation. The ECCO approximation is a major leap forward for subgroup-based self-shielding methodologies. We observe that a full correlation model, similar to the ECCO approximation, can be included in those current approaches to represent temperature gradient effects in fuel. The main improvement on radiative capture accuracy occurs in the external fuel layer where ^{239}Pu builds up. The SPM goes one step further.

It can be combined with a general correlation model based on a rigorous CALENDF probability table approach. It is therefore possible to represent explicitly the temperature distribution. Moreover, the general correlation model of the SPM was found more accurate than the full correlation model. We have compared the SPM with current methodologies and presented numerical results related to simple MOX benchmarks.

REFERENCES

De Kruijf, W. J. M. and Janssen, A. J. "The Effective Fuel Temperature to be Used for Calculating Resonance Absorption in a $^{238}UO_2$ Lump with a Nonuniform Temperature Profile," *Nucl. Sci. Eng.*, **123**, 121 (1996).

Grimstone, M. J., Tullett, J. D. and Rimpault, G. "Accurate Treatments of Fast Reactor Fuel Assembly Heterogeneity with the ECCO Cell Code." *Proc. Int. Conf. on the Physics of Reactors: Operation, Design and Computation -- PHYSOR 90*, Marseille, France, p. IX:24, April 23-27 (1990).

Hébert, Alain and Marleau, Guy. "Generalization of the Stamm'ler Method for the Self-Shielding of Resonant Isotopes in Arbitrary Geometries," *Nucl.~Sci.~Eng.*, **108**, 230 (1991).

Hébert, Alain and Coste, Mireille. "Computing Moment-Based Probability Tables for Self-Shielding Calculations in Lattice Codes." *Nucl. Sci. Eng.*, **142**, 245–257 (2002).

Hébert, Alain. "The Ribon Extended Self-Shielding Model." *Nucl. Sci. Eng.*, **151**, 1–24 (2005).

Hébert, Alain. "Towards Version4." *Proc. of Int. Mtg. on the Physics of Fuel Cycles and Advanced Nuclear Systems: Advances in Nuclear Analysis and Simulation PHYSOR 2006*, Vancouver, Canada, (2006).

Hébert, Alain. "Development of the subgroup projection method for resonance self-shielding calculations." *Nucl. Sci. Eng.*, **162**, 56–75 (2009).

Hébert, Alain. "Applied Reactor Physics." Presses Internationales Polytechniques , Montréal (2009). See the website at http://www.polymtl.ca/pub/.

Marleau, Guy, Hébert, Alain and Roy, Robert. "A User's Guide for DRAGON, Version DRAGON Release 4.00." Report IGE-174, Institut de Genie Nucléaire, Ecole

Polytechnique de Montréal, Montréal (2006). Dragon can be downloaded from the website at http://www.polymtl.ca/merlin/.

Perruchot-Triboulet, Sophie. "Validation et extensions du module d'autoprotection du code de transport neutronique multigroupe APOLLO2," Ph. D. Thesis, Université d'Aix-Marseille, Marseille (1996).

Rowlands, John *et al.* "LWR Pin Cell Benchmark Intercomparisons. An Intercomparison study organized by the JEF Project, with contributions by Britain, France, Germany, The Netherlands, Slovenia and the USA.," *JEF Report to be published* , OECD/NEA Data Bank (1999).